DMD Fast Forward. Published on January 31, 2019 as DOI: 10.1124/dmd.118.084210
This article has not been copyedited and formatted. The final version may differ from this version.

Manuscript title: *(Drug Metabolism and Disposition)*

Brain distribution of a panel of EGFR inhibitors using cassette-dosing in wild-type and *Abcb1/Abcg2* deficient mice

Authors and affiliations

Minjee Kim[1], Janice K. Laramy[1], Afroz S. Mohammad[1], Surabhi Talele[1], James Fisher[2], Jann N. Sarkaria[3] and William F. Elmquist[1]

[1]Brain Barriers Research Center, Department of Pharmaceutics, College of Pharmacy, University of Minnesota, Minneapolis, Minnesota, USA (MK, JKL, ASM, ST, WFE)

[2]Clinical Pharmacology and Analytical Services Laboratory, Department of Experimental and Clinical Pharmacology, University of Minnesota, Minneapolis, MN, USA (JF)

[3]Radiation Oncology, Mayo Clinic, Rochester, Minnesota, USA (JNS)

DMD Fast Forward. Published on January 31, 2019 as DOI: 10.1124/dmd.118.084210
This article has not been copyedited and formatted. The final version may differ from this version.

Running title

Brain distributional kinetics of EGFR inhibitors

Corresponding author

William F. Elmquist

Professor

Department of Pharmaceutics

University of Minnesota

308 Harvard ST SE

Minneapolis MN 55455

Phone: 612-625-0097; fax: 612-626-2125

e-mail: elmqu011@umn.edu

Number of pages

Number of text pages: 27

Number of tables: 6

Number of figures: 4

Number of references: 53

Number of words in abstract: 224

Number of words in introduction: (excluding in-text citations) 898

Number of words in discussion: (excluding in-text citations) 1743

Abbreviations

AUC, area under the curve

BBB, blood-brain barrier

BCRP, breast cancer resistance protein

CL, clearance

CL/F, apparent clearance

CNS, central nervous system

DMD Fast Forward. Published on January 31, 2019 as DOI: 10.1124/dmd.118.084210
This article has not been copyedited and formatted. The final version may differ from this version.

DA, distribution advantage

EGFR, Epidermal growth factor receptor

FVB, Friend leukemia virus strain B

GBM, glioblastoma

IC, intracranial

IC_{50}, the half maximal inhibitory concentration

Kp, brain-to-plasma ratio

$Kpuu_{, brain}$ unbound (free) brain-to-plasma ratio

LC-MS/MS, liquid chromatography–tandem mass spectrometry

Mdr1, Multi-drug resistance protein 1 (p-glycoprotein)

NCA, noncompartmental analysis

P-gp, P-glycoprotein

ABSTRACT (<250 words)

Tyrosine kinase inhibitors that target the epidermal growth factor receptor (EGFR) have had success in treating EGFR positive tumors, including non-small cell lung cancer (NSCLC). However, developing EGFR inhibitors that can be delivered to the brain remains a challenge. To identify optimal compounds for brain delivery, 8 EGFR inhibitors (including afatinib, AEE788, AZD3759, erlotinib, dacomitinib, gefitinib, osimertinib, and vandetanib) were evaluated for distributional kinetics using cassette dosing with the ultimate goal of understanding the brain penetrability of compounds that share the same molecular target in an important oncogenic signaling pathway for both primary brain tumors (glioblastoma) and brain metastases (e.g., NSCLC). Cassette dosing was validated by comparing the brain-to-plasma ratios obtained from cassette dosing to discrete dosing studies. The brain to blood partition coefficients (Kp,brain) were calculated following cassette dosing of the 8 EGFR inhibitors. The comparison of Kp,brain in wild-type and transporter-deficient mice confirmed that two major efflux transporters at the BBB, p-glycoprotein (P-gp) and breast cancer resistance protein (Bcrp), play a crucial role in the brain distribution of 7 out of 8 EGFR inhibitors. Results show that the prediction of brain distribution based on physicochemical properties of a drug can be misleading, especially for compounds subject to extensive efflux transport. Moreover, this study informs the choice of EGFR inhibitors, i.e., determining BBB permeability combined with a known target potency, that may be effective in future clinical trials for brain tumors.

INTRODUCTION

The epidermal growth factor receptor (EGFR) has been a useful biomarker and an attractive drug target in the treatment of various tumors (Doroshow, 2005; Seshacharyulu et al., 2012). EGFR is often found to be constitutively activated due to gene mutation and/or amplification, leading to typical oncogenic behavior, including, increased cell survival, proliferation, and invasion (Bertotti et al., 2009; Seshacharyulu et al., 2012). EGFR-tyrosine kinase inhibitors (TKIs) have been developed for use as first-line therapies for patients, especially those with non-small cell lung cancer (NSCLC), and they have shown promising efficacy in patient populations that overexpress EGFR (Doroshow, 2005). Patients with NSCLC have a substantial risk of developing metastases in central nervous system (CNS) (Rangachari et al., 2015; McCoach et al., 2016). CNS metastases often develop even when extracranial disease sites are controlled using standard regimens. First generation of EGFR inhibitors, erlotinib and gefitinib, have shown some success in treating NSCLS patients with peripheral lesions, but these drugs have had limited success in treating brain metastases of NSCLC, potentially due to limited delivery to the CNS (Kawamura et al., 2009; Agarwal et al., 2010; Weber et al., 2011; de Vries et al., 2012; Agarwal et al., 2013). Therefore, there has been a great interest in developing brain penetrant EGFR inhibitors for treating brain metastases.

While there is a clear rationale to use EGFR inhibitors in treating brain metastases, there has also been great interest in treating primary brain tumors with EGFR inhibitors. Approximately 60% of glioblastoma, the most common and aggressive type of primary brain tumor, is often found to have EGFR overexpression (approximately 60%) (Ohgaki and Kleihues, 2007; Huang et al., 2009; Brennan et al., 2013). Moreover, overexpression of EGFR is closely related to a more aggressive glioblastoma phenotype (Shinojima et al., 2003). In spite of that, EGFR inhibitors have shown no significant benefit in glioblastoma patients (Rich et al., 2004; van den Bent et al., 2009), and have not led to regulatory approval of any EGFR inhibitor for the

treatment of glioblastoma. One important factor to consider in examining reasons for the limited efficacy of these drugs in the CNS is that the delivery of many early EGFR inhibitors has shown to be insufficient to elicit a response at the target site in the CNS. Moreover, many of the early generation inhibitors are substrates of the major efflux transporters, p-glycoprotein (P-gp) and breast cancer resistance protein (Bcrp), that at the blood-brain barrier (BBB), may lead to limited brain penetration, especially in intra-tumoral regions that have an intact BBB in metastases (Lockman et al., 2010) and primary tumor (Sarkaria et al., 2018).

In the current study, we examined the distribution to the brain of a set of EGFR inhibitors, including early generation inhibitors, erlotinib, gefitinib and afatinib, and more recently developed inhibitors, osimertinib, vandetanib, AZD3759, dacomitinib, and AEE877 (Figure 1 and Table 1). These eight EGFR inhibitors were chosen based on previous and possible future use in patients with brain tumors. In addition, based on the few preclinical studies with these drugs, this series of EGFR inhibitors was chosen with the intention of having a wide range of BBB permeability.

Brain distributional kinetics were examined by using a cassette-dosing strategy. Cassette-dosing studies are typically performed by co-administering a low dose of multiple compounds to a single animal to calculate pharmacokinetic parameters and metrics of individual compounds from the concentration-time pharmacokinetic profile (Manitpisitkul and White, 2004). As such, multiple concentration-time profiles of individual drugs can be obtained in a single animal. One of the benefits of using cassette dosing strategy is that throughput of the study is significantly increased and the number of animals that are used for the study is significantly reduced. This is especially true in pharmacokinetic and brain distribution studies with mice that are often conducted using a destructive sampling strategy, and may require numerous animals for a single study with a single agent. Another interesting aspect of using cassette dosing to determine the CNS distribution of a series of compounds is that the brain penetration of different

compounds can be examined within a single animal under the identical physiological conditions, including blood flow, BBB surface area, tight junction integrity, transporter expression and function. The most common concern with cassette dosing strategy is regarding the possibility of drug-drug interactions due to coadministration of multiple drugs at the same time. However, several studies have reported that drug-drug interactions at the BBB are unlikely to happen in cassette dosing, due to low dosages used in the study (1-2 mg/kg) (Manitpisitkul and White, 2004; Liu et al., 2012) relative to the capacity of the transport systems (Cordon-Cardo et al., 1989; Cooray et al., 2002).

We examined the extent of brain penetration of these 8 EGFR inhibitors by calculating AUC ratios in brain and plasma following cassette dosing. To ensure there were no drug-drug interactions at the BBB, we also performed discrete dosing studies for individual drugs and compared the brain-to-plasma ratios at two time points (1-hr and 8-hr post dose) with the results from the cassette dosing study. Pharmacokinetic parameters and metrics were calculated from concentration-time profiles of each drug from cassette dosing studies. The correlation between the CNS multiparameter optimization (MPO) score (Wager et al., 2010; Wager et al., 2016) and the measured brain penetration of these compounds was examined in order to determine the relationship between various physicochemical properties taken together in a series of EGFR inhibitors.

DMD Fast Forward. Published on January 31, 2019 as DOI: 10.1124/dmd.118.084210
This article has not been copyedited and formatted. The final version may differ from this version.

MATERIALS AND METHODS

Chemicals and reagents

6-[4-[(4-ethylpiperazin-1-yl)methyl]phenyl]-N-(1-phenylethyl)-7H-pyrrolo[2,3-d]pyrimidin-4-amine (AEE788) and [4-(3-chloro-2-fluoroanilino)-7-methoxyquinazolin-6-yl] (2R)-2,4-dimethylpiperazine-1-carboxylate (AZD3759) were purchased from Selleck Chemicals (Houston, TX). N-[2-[2-(dimethylamino)ethyl-methylamino]-4-methoxy-5-[[4-(1-methylindol-3-yl)pyrimidin-2-yl]amino]phenyl]prop-2-enamide (osimertinib), N-(3-chloro-4-fluorophenyl)-7-methoxy-6-(3-morpholin-4-ylpropoxy)quinazolin-4-amine (gefitinib), N-(4-bromo-2-fluorophenyl)-6-methoxy-7-[(1-methylpiperidin-4-yl)methoxy]quinazolin-4-amine (vandetanib), N-(3-ethynylphenyl)-6,7-bis(2-methoxyethoxy)quinazolin-4-amine;hydrochloride (erlotinib hydrochloride), and (E)-N-[4-(3-chloro-4-fluoroanilino)-7-methoxyquinazolin-6-yl]-4-piperidin-1-ylbut-2-enamide (dacomitinib) were purchased from LC laboratories (Woburn, MA). (E)-N-[4-(3-chloro-4-fluoroanilino)-7-[(3S)-oxolan-3-yl]oxyquinazolin-6-yl]-4-(dimethylamino)but-2-enamide (Afatinib), [13C, 2H3]-osimertinib, [2H6]-gefitinib, [13C, 2H6]-vandetanib, [2H6]-erlotinib HCL, and [2H6]-afatinib were purchased from Alsachim SAS (Illkirch, France). Analytic-grade reagents were purchased from Fisher Scientific (Waltham, MA). The rapid equilibrium dialysis (RED) device, including a 96-well base plate and membrane inserts (8 kDa molecular weight cut-off cellulose dialysis membrane), was purchased from Thermo Fisher Scientific Inc. (Waltham, MA).

Animals

Animals for pharmacokinetic studies and in vitro binding assays utilized both female and male Friend leukemia virus strain B (FVB) wild-type and Mdr1a/b$^{-/-}$Bcrp1$^{-/-}$ mice (Taconic Biosciences, Inc., Germantown, NY) at the age of 8-14 weeks. Animals were bred and

maintained in the accredited research animal housing facility at the University of Minnesota. Transgenic mouse colonies were routinely validated by conducting tail snip followed by genotyping (TransnetYX, Cordova, TN). All protocols for the animal experiments were approved by University of Minnesota Institutional Animal Care and Use Committee (IACUC) and performed in accordance with the Guide for the Care and Use of Laboratory Animals by the U.S. National Institutes of Health (Bethesda, MD).

Discrete Dosing Pharmacokinetic Study

The dosing suspensions for subcutaneous injection were prepared in 10 % DMSO and 0.25% hydroxypropyl methylcellulose (w/v) in order to achieve a dose of 1 mg/kg for each EGFR inhibitor. A single dose of each EGFR inhibitor was individually dosed in wild-type and triple knockout (*Mdr1a/b*$^{-/-}$*Bcrp1*$^{-/-}$) FVB mice. Blood and brain samples from mice were harvested at 1-hour and 8-hour after discrete drug administration (*N*=3-4 at each time point). Blood was collected by cardiac puncture using heparinized syringes after euthanizing in a carbon dioxide chamber. Plasma was separated by centrifuge at 6500 rpm at 4 °C for 20 minutes. Both plasma and brain samples were stored at -80 °C until LC-MS/MS analysis.

Cassette Dosing Pharmacokinetic Study

The dosing suspension for cassette dosing was prepared in the final strength of 10% DMSO and 0.25% hydroxypropyl methylcellulose (w/v) the same way for discrete dosing to make the mixture of 8 EGFR inhibitors in the final dosing suspension of 1 mg/kg. A single cocktail of 8 EGFR inhibitors was administered by subcutaneous injection in wild-type and triple knockout (*Mdr1a/b*$^{-/-}$*Bcrp1*$^{-/-}$) FVB mice. Blood and brain samples were harvested at pre-determined

time points, including 0.5, 1, 2, 4, 8, and 16 hours after dosing (*N*=3-4 at each time point). Blood and plasma were collected and separated as described in the discrete dosing study.

Protein Binding Study in Plasma and Brain Homogenate

The free fractions of EGFR inhibitors were determined by using a rapid equilibrium dialysis (RED) device. Mouse plasma was obtained from FVB mice by cardiac puncture. The brain homogenate was prepared from FVB mouse by adding 2 volumes (w/v) of phosphate buffered saline (PBS; pH 7.4) followed by mechanical homogenization. EGFR inhibitor stock solutions are prepared in DMSO, and added to either mouse plasma or brain homogenate to make a final concentration of 5 μM containing 0.3% DMSO. Either mouse plasma or brain homogenate containing compounds was loaded to the sample chamber (300 μl) of the inserts first, and then blank PBS was loaded to the corresponding buffer chamber (500 μl) according to the manufacturer's instruction (N=4). The plate was sealed with an adhesive lid and incubated at 37 °C for 4 hours in an orbital shaker at 300 rpm. Samples were collected from both chambers after the incubation, and stored in -80°C freezer until LC-MS/MS analysis.

Unbound free fractions in the brain were calculated according to the following equation (Kalvass and Maurer, 2002):

$$\text{Free fraction (fu)} = \frac{1/D}{\left(\left(\frac{1}{fu,diluted}\right)-1\right)+1/D} \qquad (1).$$

The dilution factor (D) was 3 in the experiment described above.

The unbound (free) concentration partitioning to the brain was determined as below:

$$\text{Free brain partition coefficient (Kp,uu)} = \frac{\text{free brain concentration}}{\text{free plasma concentration}} = K_{p,\,brain} \times \frac{fu_{,brain}}{fu_{,plasma}} \qquad (2),$$

where $K,p_{\,brain}$ is the ratio of brain-to-plasma areas under the total concentration time profile as below:

DMD Fast Forward. Published on January 31, 2019 as DOI: 10.1124/dmd.118.084210
This article has not been copyedited and formatted. The final version may differ from this version.

$$\text{Brain partition coefficient } (K_{p,\,brain}) = \frac{AUC_{\,brain}}{AUC_{\,plasma}} \qquad (3).$$

The distribution advantage (DA) due to the lack of efflux transporters was calculated as below:

$$\text{Distribution advantage (DA)} = \frac{Kp_{\,brain,\,transporter\ knockout\ mice}}{Kp_{\,brain,\,wild\text{-}type\ mice}} \qquad (4)$$

Analytical LC-MS/MS analysis to determine drug concentrations

Concentrations of the 8 EGFR inhibitors in specimens were measured using reverse-phase liquid chromatography (Agilent model 1200 separation system; Agilent Technologies, Santa Clara, CA) coupled with TSQ Quantum triple quadruple mass spectrometer (Thermo Finnigan, San Jose, CA) by operating electrospray in the positive ion mode. For liquid chromatographic separation, either gradient or isocratic elution was performed using Phenomenex Synergi Polar-RP column (75 X 2 mm, 4 μm; Phenomenex) depending on the compounds. The initial composition of mobile phase for AEE788, AZD3759, afatinib, and gefitinib was comprised of 75% distilled water with 0.1% formic acid (A) and 25% acetonitrile with 0.1% formic acid (B) with a 0.35 ml/min flow rate. The total run time was 7.5 minutes. The retention times for AEE788, AZD3759, afatinib, and gefitinib were 1.01, 1.30, 1.00, and 1.43 minutes, respectively. The initial mobile phase composition for osimertinib, erlotinib, and vandetanib was comprised of 70% distilled water with 0.1% formic acid (A) and 30% acetonitrile with 0.1% formic acid (B) with a 0.35 ml/min flow rate. The total run time was 8.5 minutes. The retention times for osimertinib, erlotinib, and vandetanib were 1.06, 3.54, and 0.73 minutes, respectively. An isocratic separation was performed to separate dacomitinib with the initial condition of 70% aqueous phase (A) and 30% organic phase (B) for 4 minutes. The retention time for dacomitinib was 0.85 minutes. Mass-to-charge ratio (m/z) transitions were as follows: 500.14 > 72.15 for osimertinib, 504.14 > 72.14 for [^{13}C, $^{2}H_3$]-osimertinib, 460.1 > 141.16 for AZD3759, 447.1 >

DMD Fast Forward. Published on January 31, 2019 as DOI: 10.1124/dmd.118.084210
This article has not been copyedited and formatted. The final version may differ from this version.

128.2 for gefitinib, 455.1 > 136.2 for [$^{2}H_{8}$]-gefitinib, 475.1 > 112.1 for vandetanib, 481 > 112.1 for [^{13}C, $^{2}H_{6}$]-vandetanib, 394.1 > 278 for erlotinib, 400.1 > 284 for [^{13}C]-erlotinib, 486.1 > 371.1 for afatinib, 492.1 > 377.1 for [$^{2}H_{6}$]-afatinib, 441.27 > 223.05 for AEE788, and 470.2 > 385.0 for dacomitinib.

Pharmacokinetic Calculations

Plasma and brain concentration-time data were analyzed with non-compartmental analysis (NCA) using Phoenix WinNonlin version 8.0 (Certara USA, Inc., Princeton, NJ). Areas under the curve (AUCs) for each compound were calculated by the trapezoidal rule to the last time point ($AUC_{(0\rightarrow tlast)}$). Other pharmacokinetic parameters/metrics, including clearance (CL), volume of distribution (Vd), and half-life were determined by NCA. Brain-to-plasma ratios (Kp) of each EGFR inhibitor were calculated by the ratio of $AUC_{(0\rightarrow tlast)}$ of brain concentration-time profile ($AUC_{(0\rightarrow tlast),\ brain}$) to that of plasma concentration-time profile ($AUC_{(0\rightarrow tlast),\ plasma}$). Free partition coefficients of brain (Kp,uu) were calculated by multiplying the Kp with the ratio of free fraction in brain homogenate to plasma ($f_{u,brain}/f_{u,plasma}$). A brain distribution advantage (DA) in triple knock-out mice, that are lacking both P-gp and Bcrp (*Mdr1a/b*$^{-/-}$*Bcrp1*$^{-/-}$), compared to wild-type mice was obtained by calculating the ratio of Kp in triple knock-out to wild-type mice.

Statistical Testing

All data are presented as mean ± standard deviation (S.D) or standard error of an estimate (S.E.). To compare the brain to plasma ratio in cassette dosing to that in discrete dosing, a pairwise multiple t-test was performed by using GraphPad Prism (version 6; GraphPad

Software, La Jolla California USA). A significance level at $P < 0.05$ was considered as a statistically significant difference in all statistical testing.

RESULTS

Comparison of brain-to-plasma ratios from cassette and discrete dosing studies.

The brain-to-plasma ratios of each drug at a 1-hour and 8-hour following cassette dosing studies were compared with the results from discrete dosing studies at the same times post dose in both wild-type and TKO mice (Figure 2). Figure 2A shows the brain-to-plasma ratios of the 8 EGFR inhibitors from cassette dosing are within two-fold of the ratios from discrete dosing in wild-type mice at 1-hour after dosing, except AEE788, which shows higher brain-to-plasma ratio following discrete dosing than in cassette dosing (* $P<0.05$). Likewise, at 8-hour after dosing in wild-type mice, 5 out of 7 compounds are within two-fold difference in cassette dosing study when compared to discrete dosing study (Figure 2B). The two exceptions, afatinib and osimertinib, show a slightly higher brain-to-plasma ratio in cassette dosing study than in discrete dosing study (afatinib: * $P<0.05$, osimertinib: *N.S.*). In TKO mice, brain-to-plasma ratios of these drugs from cassette dosing study matched well with the results from discrete dosing study, except AEE788 at 8-hour post dose (Figure 2C and 2D, * $P<0.05$). Overall, the results from cassette dosing study show good agreement with those from discrete dosing studies. Even though there were some values that are out of the two-fold range, the brain to plasma ratios from cassette and discrete dosing strategy were comparable and support the use of the cassette dosing as a valid strategy to compare brain partition coefficients across the series of compounds.

DMD Fast Forward. Published on January 31, 2019 as DOI: 10.1124/dmd.118.084210
This article has not been copyedited and formatted. The final version may differ from this version.

Pharmacokinetic parameters and metrics of 8 EGFR inhibitors following cassette dosing in wild-type and *Mdr1a/b*$^{-/-}$*Bcrp1*$^{-/-}$ FVB mice.

The concentration-time profiles of 8 EGFR inhibitors following a single cassette dosing by subcutaneous injection were used to calculate pharmacokinetic parameters and metrics by using non-compartmental analysis (NCA) in WT and TKO (Table 2 and Table 3). Half-life of inhibitors in plasma were calculated based on the concentrations of plasma at the last three or four time points in the concentration-time profile where the drugs were in elimination phase. Half-life of these drug are ranging from 50 minutes with erlotinib to 13.7 hours with vandetanib in wild-type FVB mice, and from 50 minutes with erlotinib to 17.6 hours with AEE788 in triple-knockout (Mdr1a/b–/–Bcrp1–/–) FVB mice. When the half-life of each drug in wild-type FVB mice is compared to the values in knockout animals, 7 out of 8 inhibitors have shown similar values within a 2-fold difference. Vandetanib showed differences over 2-fold in triple-knockout (TKO) FVB mice (5.74) when compared to wild-type mice (13.7), and the AUC in wild-type FVB mice was significantly higher than that in TKO mice (2230 $\pm$ 61.3 (WT) vs. 1442 $\pm$ 98.7 (TKO), $^{*}P < 0.05$). Based on the non-compartmental analysis for vandetanib, the apparent volume of distribution (Vd/F) in WT was comparable to TKO (4947 mL/kg (WT) vs. 5085 mL/kg (TKO)), but the apparent clearance (CL/F) in TKO was about 2.5-fold higher than the value in WT (250 mL/hr/kg (WT) vs. 614 mL/hr/kg (TKO)). Except vandetanib, all other inhibitors have shown similar plasma AUCs in wild-type when compared to TKO mice. Overall, half-lives of these inhibitors in the brain were close to half-lives observed in plasma. Gefitinib and Afatinib in wild-type mice, and vandetanib in TKO, were the exceptions that showed longer half-life in brain than in plasma. Overall, systemic pharmacokinetic parameters and metrics in WT were similar to the values in TKO, but the AUC in brain were markedly different in WT and TKO across all compounds, following a cassette dosing of a set of EGFR inhibitors (concentration-time profiles of each drug is available in supplemental figure 1 and 2).

Brain penetration of EGFR inhibitors within an individual animal

The brain penetration of each EGFR inhibitor following cassette dosing was examined by calculating the brain-to-plasma ratio of each compound at each time point, within individual animal subjects. This allowed these compounds to be rank ordered from the highest penetration (high brain-to-plasma ratio) to the lowest penetration (low brain-to-plasma ratio) within a single animal subject. Ranked values within the same subjects were color-coded depending on their brain penetration in Figure 3, where dark blue was used for a compound with the highest brain penetration and dark red was used for the drugs with the lowest brain penetration. When the measured concentration was lower than the lowest limit of quantitation, the "penetration" color was greyed and marked as LLOQ. This "visual heat-map" of the rank order of the brain penetration of inhibitors was consistent across different subjects at different time points in both wild-type and triple-knockout mice. The overall classification of brain penetration, defined with color, either in the blue group or the red group, was consistent especially at the same time point after dosing. Interestingly, these rank orders within a mouse are more consistent across mice at early time points, until approximately 2 hours after cassette dosing, and less consistent at later time points in both WT and TKO animals.

Determination of Kp and Kpuu for brain

The partition coefficients (Kp) of brain for this set of EGFR inhibitors were determined in both wild-type and TKO FVB mice from the cassette dosing study (Table 4 and supplemental figure 3). The brain partition coefficients were calculated by the ratios of AUC of brain total concentration-time profile to AUC of plasma concentration-time profile from time zero to the last time point of measured concentrations (16-hour). In wild-type mice that have intact efflux transporters in the BBB, the brain Kp was the highest for AZD3759 (1.7) and the lowest for erlotinib and AEE788 (0.062 and 0.066, respectively). These Kp values were increased in TKO mice for all studied compounds when compared to wild-type mice. However, the relative

DMD Fast Forward. Published on January 31, 2019 as DOI: 10.1124/dmd.118.084210
This article has not been copyedited and formatted. The final version may differ from this version.

magnitude of increase in Kp was highly variable, from 1.6-fold for AZD3759 up to 28-fold for AEE788, as quantified by distribution advantage (DA) with equation (4) as shown in Table 4. The free fractions of these compounds were determined in mouse plasma and brain homogenate using rapid equilibrium dialysis. The free partition coefficients of brain (Kp,uu) are presented in Table 4. Kp and Kp,uu values were the highest with AZD3759 in wild-type mice. Kp was the lowest with erlotinib in wild-type, while, Kp,uu was the lowest with AEE788 in wild-type mice. Importantly, in the wild-type mice, most of the Kp,uu values were well below unity, indicating that efflux system(s) play a significant role in limiting the brain penetration of these EGFR inhibitors. AZD3759 was the only compound that showed Kp,uu higher than unity (i.e., 2.96), indicative of a possible involvement of an influx system on modulating the delivery of this compound across the BBB. The rank orders of Kp and Kp,uu values showed that osimertinib has the highest Kp in TKO mice (15.7), which is about 16-fold higher than in wild-type mice. Although the rank orders of these values were changing depending on not only the degree of binding in plasma and brain but also the presence and the absence of efflux transporters, AZD3759, osimertinib, vandetanib, and dacomitinib consistently ranked with a comparatively high brain penetration. On the other hand, the other four compounds in this cassette of eight EGFR inhibitors, including erlotinib, AEE788, afatinib, and gefitinib, categorized in the low brain penetration group.

Correlation between physicochemical properties and the brain partition coefficients

Correlations between physicochemical properties and the brain penetration of this set of EGFR inhibitors were examined. A calculated CNS multiparameter optimization (MPO) score (Wager et al., 2010) and the ratios of cLogD to square root of molecular weight (clogD/sqrt(MW)) (Levin, 1980) were compared to Kp brain and Kp,uu in wild-type and TKO mice (Table 5 and Figure 4). The suggested CNS MPO scores are typically higher than 4 to predict good CNS penetration

(Wager et al., 2016), and the MPO scores for the series of EGFR inhibitors were calculated by the most recent version of MPO score calculation tool (Wager et al., 2016). Importantly, using this tool, dacomitinib, vandetanib, and osimertinib were classified as low brain penetrants according to their MPO scores, but erlotinib and gefitinib as high brain penetrants. On the other hand, the method of predicting brain penetration of compounds by using the ratios of cLogD to square root of molecular weight predicted dacomitinib, vandetanib, and AEE788 as high brain penetrants, and erlotinib as a low brain penetrant. Based on the experimentally-determined brain partition coefficients (Kps) reported above from our cassette dosing studies, osimertinib, dacomitinib, and vandetanib were consistently classified as high brain penetrants in wild-type FVB mice, and erlotinib and gefitinib as low brain penetrants. Moreover, compounds with similar MPO scores, for example, AEE788 (3.3) and vandetanib (3.3), have widely different Kp values in wild-type mice, ranging from 0.635 for vandetanib, classified as highly brain penetrant, to 0.066 for AEE788, classified as a low brain penetrant (Table 5 and Figure 4C). A similar pattern was observed with cLogD/sqrt(MW) in AEE788, dacomitinib, and erlotinib, that each have close cLogD/sqrt(MW) values, but Kp values that are considerably different from one another. The free partition coefficients of brain (Kp,uu) were plotted against either cLogD/sqrt(MW) or MPO scores to understand the influence of binding in these correlations, however, no improved correlation was seen in these parameters (Figure 4). When the effect of major transporters, P-gp and Bcrp, was absent using TKO mice, the $Kp_{,brain}$ seemed to have a modest correlation with cLogD/sqrt(MW), but no correlation with MPO scores (Figure 4B and 4D). In conclusion, both cLogD/sqrt(MW) and MPO score fail to show a clear predictive correlation with either $Kp_{,brain}$ or $Kp,uu_{,brain}$. About half of compounds show a weak correlation between their physicochemical properties and brain distribution, whereas the other half showed no correlation.

Discussion

Epidermal growth factor receptor (EGFR) has been an attractive target for treatment of primary brain tumors including glioblastoma (GBM), in which EGFR is over-expressed in about 60% of patients (Ohgaki and Kleihues, 2007; Huang et al., 2009; Brennan et al., 2013), as well as brain metastases from various cancers. However, one of the major challenges in developing an efficacious anticancer drug for tumors located in the brain is "delivery" of these agents to the site of action, the brain tumor across an often intact blood-brain barrier (BBB). A brain-to-blood partition coefficient (Kp,brain) is commonly used to experimentally determine and describe the brain distribution of a drug, requiring animal experiments. Recently, other methods, including a cassette dosing strategy (*N*-in-1 dosing), as well as prediction methods based on various physicochemical properties of a compound, have been suggested to determine or predict the brain distribution of therapeutics, which can possibly replace the experimental processes, especially in discovery and development of brain penetrant compounds. The present study shows that the cassette dosing approach can be useful to determine brain penetration of a series of compounds with the same pharmacological target, and to understand a role of efflux transporters at the BBB on the brain distribution of these small molecule therapeutics.

In the current study, we chose 8 EGFR inhibitors that are in different stages of clinical development and varying in their known brain penetration. 5 out of 8 EGFR inhibitors, including afatinib, erlotinib, gefitinib, osimertinib, and vandetanib, are approved anticancer drugs for various solid tumors, including non-small cell lung cancer (NSCLC), a tumor that often metatasizes to the brain. However, none of these approved first and second generation of EGFR inhibitors are effective in patients with primary brain tumors, and have modest and variable efficacy in patients with metastatic brain tumors (Table 6), possibly due to their limited brain delivery across an intact blood-brain barrier. Therefore, there has been a critical need to develop a CNS penetrant EGFR inhibitor. Dacomitinib and AZD3759 are third generation of

EGFR inhibitors. AZD3759 and osimertinib are reported to be CNS penetrating EGFR inhibitors that are under clinical investigation for the treatment of advanced NSCLC. Clinical studies with AZD3759 demonstrate an objective response rate in over 80% of patients with NSCLC brain metastases (Ahn et al., 2017). Osimertinib has also shown promise in treating brain metatases (Goss et al., 2018). Dacomitinib has some limited efficacy in patients with metastatic NSCLC brain tumors harboring the T790M mutation (NCT01858389), and its efficacy in GBM is currently under clinical investigation (NSC01112527).

It is possible that irreversible inhibitors, including dacomitinib, afatinib, and osimertinib, may not need as high brain partitioning as for reversible inhibitors in order to achieve the same pharmacodynamic effect. This is predicated on the turnover of the drug-receptor complex. If an EGFR-inhibitor – receptor complex is rapidly turned over, the benefit of being an irreversile inhibitor can be lost. As such, it is still valuable to assess the ability of CNS penetration of all of these drugs, both reversible and irreversible inhibitors, to predict potential efficacy in brain tumor.

The comparison of brain to plasma ratios determined by both cassette and discrete dosing confirms the absence of drug-drug interactions at the BBB in this series of compounds similar to that reported previously by Liu et al (Liu et al., 2012). In the current study, brain to plasma ratios of a series of EGFR inhibitors obtained at 1 and 8 hours after dosing as a cassette were within a 2-fold range of the results from discrete dosing in both wild-type and transgenic mice that are lacking both P-glycoprotein (P-gp) and breast cancer resistance protein (Bcrp) (TKO). The greatest difference in brain to plasma ratio between cassette and discrete dosing was observed with afatinib at 8 hour after dosing in wild-type mice, where the brain to plasma ratio estimate from the cassette study was about 5 times overestimated than the value from discrete dosing. On the other hand, brain to plasma ratios of AEE788 after cassette dosing underestimated the values after discrete dosing at 1 hour post dose in wild-type mice and at 8

hour post dose in TKO mice. There were no consistent trends between these outliers, and therefore this may represent experimental variability rather than a systematic trend related to the dosing strategies. Although both afatinib and AEE788 seem to be substrates of both P-gp and Bcrp, recognized from the values of the distribution advantage (DA) for these compounds, other compounds that are substrates of P-gp and Bcrp do not show any discrepancy between the results from cassette and discrete studies. In conclusion, overall the results from cassette dosing match well with the results from discrete dosing. Thus, the close correlation between cassette and discrete dosing results confirm that there are no significant drug-drug interactions occurring at the BBB, with the dose of 1 mg/kg, regardless of the efflux transporter liability.

The partition coefficients of brain (Kp,brain) for each EGFR inhibitor were calculated from the AUC ratios of brain to plasma. In the current study, AUCs from time zero to the last time point were used for both plasma and brain without the extrapolation of AUC from the last time point to infinity, because the complete elimination phase was not reached until 16 hours after the dosing for some compounds. Therefore, AUCs from time zero to the last time point that concentrations were measured (i.e., 4 hours after the dosing for erlotinib, 16 hours after the dosing for all other compounds) were used for both plasma and brain to calculate the Kp,brain for each EGFR inhibitors. When the calculated Kp,brain from this study were compared with previously reported Kp,brain (Table 5), values were within 2-fold, except for vandetanib. Based on a Kp,brain in wild-type mice over 0.5, AZD3759, dacomitinib, osimertinib, and vandetanib can be classified as brain penetrant EGFR inhibitors.

The free partition coefficients were calculated with the free fractions in plasma and brain homogenate determined by rapid equilibrium dialysis in the current study. According to our findings, four compounds that have the highest free brain partition coefficients were the brain penetrant EGFR inhibitors based on their Kp,brain, even though the order of the values were slightly different from the total concentration based Kp,brain. The equilibrium dialysis is one of

the most common way to determine the free fractions of compounds, and the most efficient method with reasonable predictability (Becker and Liu, 2006). However, there has been a concern about non-specific adsorption to the device especially the compounds with low free fractions (Riccardi et al., 2015), and a novel method to determine the free fractions in highly bound compounds has been proposed recently (Kalvass et al., 2018). Therefore, considering the limitations with the current method used in the study, the further evaluations of the free fractions and Kp,uu for these 8 EGFR inhibitors are needed by using different methods.

Previous research on the efflux transporter liability of these EGFR inhibitors have shown that afatinib, erlotinib, gefitinib, osimertinib, and vandetanib are substrates of both P-gp and Bcrp (Agarwal et al., 2010; Minocha et al., 2012; Agarwal et al., 2013; Ballard et al., 2016). On the other hand, AZD3759 has been reported to not be a substrate of both P-gp and Bcrp. The Kp,brain calculated in the current study agree with the previous results in that the compounds known to be substrates of efflux transporters showed much higher brain partition coefficient values in Mdr1a/b$^{-/-}$Bcrp1$^{-/-}$ mice (TKO) when compared to wild-type mice. AEE788 and dacomitinib, which have no previous reports regarding their efflux transporter liability, are shown in this study to be substrates of both/either P-gp and/or Bcrp (see the DA values, Table 4). The Kp,brain in TKO for AZD3759 was similar to the value in wild-type with the distribution advantage (DA) of 1.56, that indicates neither P-gp nor Bcrp play a major role in the brain distribution of AZD3759, as has been previously reported (Zeng et al., 2015; Yang et al., 2016). In conclusion, 7 out of 8 EGFR inhibitors investigated in the current study are shown to be substrates of both/either P-gp and Bcrp based on the DA calculated with the brain partition coefficients in wild-type and TKO mice, and AZD3759 is the only exception that is not a substrate of both P-gp and Bcrp.

The brain penetration of each EGFR inhibitor was examined within a single animal to assess the brain penetrability of each drug under the same physiological conditions by using a “visual

heatmap". Rank orders of brain-to-plasma ratios at a single time point were consistent until 2 hours after dosing in both wild-type and TKO mice. There can be several reasons of having less consistent rank orders after 2 hours. One explanation is that the systemic clearances and the brain distributional clearances, or the combination of the two, that influence the brain-to-plasma ratios may be different in individual animals, and this difference would be eccentuated at late times. Another reason can be that some compounds are somewhat excluded from the rank calculation due to low concentration measured near the lowest limit of quantitation. Importantly, the ability of each of these inhibitors to distribute into the brain within a single animal seems to be consistent between animals, even though some physiological conditions may be slightly different in each animal.

The brain distribution, including the BBB permeability of a drug, can be related to the physicochemical properties of a compound when passive diffusion dominates drug transport processes. Importantly, molecular weight, lipophilicity (logP or logD), hydrogen bond donor and acceptor count (HBD), and topological polar surface area (TPSA) of a molecule are considered to be crucial properties to determine the intrinsic permeability and brain distribution (Rankovic, 2015; Heffron, 2016). Among these crucial characteristics of a molecule, clogD and molecular size (weight) were believed to be two key factors that determine the ability to cross the BBB (Oldendorf, 1974; Levin, 1980). It has been shown that there is a reasonable correlation between the calculated ratios of clogD and square root of molecular weight and the permeability in the brain capillaries, using in situ perfusion as a measure of permeability (Levin, 1980). Recently, the central nervous system multiparameter optimization (CNS MPO) desirability tool has been proposed to predict the CNS penetration and understand the relationship between physicochemical properties and the drug distribution in CNS (Wager et al., 2010; Wager et al., 2016). In the current study, we found that there was a lack of correlation between the brain distribution of a compound defined by Kp,brain, and the physicochemical properties of a set of

EGFR inhibitors. Even if non-specific protein binding or the effect of major transporters, P-gp and Bcrp, were considered by using free partition coefficient (Kpuu) or transporter deficient mice, no predictive correlation between brain penetrability and physicochemical properties of these compounds was found (Figure 4).

In conclusion, the current study indicates that cassette dosing can be a useful method to determine the brain distribution of a set of molecularly targeted anticancer therapeutics that share the same target, in this case, EGFR. The concordance of the brain to plasma ratios at a single time point following either cassette dosing or discrete dosing has validated that both methods are comparable, especially for rank order screening. A cassette dosing strategy is useful, not only because of cost and time efficiency, but also because of the ability to directly compare drug brain penetrability among a set of compounds within a single animal. The rank orders of the brain to plasma ratios in a single animal were consistent with the rank orders of Kp,brain calculated by AUC ratios of brain to plasma. Therefore, cassette dosing strategy can be useful for candidate selection with respect to brain distribution. Among this set of EGFR inhibitors examined in the current study, AZD3759, osimertinib, vandetanib, and dacomitinib have superior brain penetration (over 50% of corresponding plasma concentration). These brain penetrant EGFR inhibitors may have value for the treatment of tumors located in the brain and should be considered for future clinical trials.

AUTHORSHIP CONTRIBUTIONS

Participated in research design: Kim, Laramy, Sarkaria, Elmquist

Conducted experiments: Kim, Laramy, Mohammad, Talele, Fisher

Performed data analysis: Kim, Sarkaria, Elmquist

Wrote or contributed to the writing of the manuscript: Kim, Sarkaria, Elmquist

REFERENCES

Agarwal S, Manchanda P, Vogelbaum MA, Ohlfest JR, and Elmquist WF (2013) Function of the blood-brain barrier and restriction of drug delivery to invasive glioma cells: findings in an orthotopic rat xenograft model of glioma. *Drug Metab Dispos* **41:**33-39.

Agarwal S, Sane R, Gallardo JL, Ohlfest JR, and Elmquist WF (2010) Distribution of gefitinib to the brain is limited by P-glycoprotein (ABCB1) and breast cancer resistance protein (ABCG2)-mediated active efflux. *J Pharmacol Exp Ther* **334:**147-155.

Ahn MJ, Kim DW, Cho BC, Kim SW, Lee JS, Ahn JS, Kim TM, Lin CC, Kim HR, John T, Kao S, Goldman JW, Su WC, Natale R, Rabbie S, Harrop B, Overend P, Yang Z, and Yang JC (2017) Activity and safety of AZD3759 in EGFR-mutant non-small-cell lung cancer with CNS metastases (BLOOM): a phase 1, open-label, dose-escalation and dose-expansion study. *Lancet Respir Med* **5:**891-902.

Ballard P, Yates JW, Yang Z, Kim DW, Yang JC, Cantarini M, Pickup K, Jordan A, Hickey M, Grist M, Box M, Johnstrom P, Varnas K, Malmquist J, Thress KS, Janne PA, and Cross D (2016) Preclinical Comparison of Osimertinib with Other EGFR-TKIs in EGFR-Mutant NSCLC Brain Metastases Models, and Early Evidence of Clinical Brain Metastases Activity. *Clin Cancer Res* **22:**5130-5140.

Becker S and Liu X (2006) Evaluation of the utility of brain slice methods to study brain penetration. *Drug Metab Dispos* **34:**855-861.

Bertotti A, Burbridge MF, Gastaldi S, Galimi F, Torti D, Medico E, Giordano S, Corso S, Rolland-Valognes G, Lockhart BP, Hickman JA, Comoglio PM, and Trusolino L (2009) Only a subset of Met-activated pathways are required to sustain oncogene addiction. *Sci Signal* **2:**ra80.

Brennan CW, Verhaak RG, McKenna A, Campos B, Noushmehr H, Salama SR, Zheng S, Chakravarty D, Sanborn JZ, Berman SH, Beroukhim R, Bernard B, Wu CJ, Genovese G, Shmulevich I, Barnholtz-Sloan J, Zou L, Vegesna R, Shukla SA, Ciriello G, Yung WK, Zhang W, Sougnez C, Mikkelsen T, Aldape K, Bigner DD, Van Meir EG, Prados M, Sloan A, Black KL, Eschbacher J, Finocchiaro G, Friedman W, Andrews DW, Guha A, Iacocca M, O'Neill BP, Foltz G, Myers J, Weisenberger DJ, Penny R, Kucherlapati R, Perou CM, Hayes DN, Gibbs R, Marra M, Mills GB, Lander E, Spellman P, Wilson R, Sander C, Weinstein J, Meyerson M, Gabriel S, Laird PW, Haussler D, Getz G, Chin L, and Network TR (2013) The somatic genomic landscape of glioblastoma. *Cell* **155:**462-477.

Ceresoli GL, Cappuzzo F, Gregorc V, Bartolini S, Crino L, and Villa E (2004) Gefitinib in patients with brain metastases from non-small-cell lung cancer: a prospective trial. *Ann Oncol* **15:**1042-1047.

Chen Y, Wang M, Zhong W, and Zhao J (2013) Pharmacokinetic and pharmacodynamic study of Gefitinib in a mouse model of non-small-cell lung carcinoma with brain metastasis. *Lung Cancer* **82:**313-318.

Cooray HC, Blackmore CG, Maskell L, and Barrand MA (2002) Localisation of breast cancer resistance protein in microvessel endothelium of human brain. *Neuroreport* **13:**2059-2063.

Cordon-Cardo C, O'Brien JP, Casals D, Rittman-Grauer L, Biedler JL, Melamed MR, and Bertino JR (1989) Multidrug-resistance gene (P-glycoprotein) is expressed by endothelial cells at blood-brain barrier sites. *Proc Natl Acad Sci U S A* **86:**695-698.

Cross DA, Ashton SE, Ghiorghiu S, Eberlein C, Nebhan CA, Spitzler PJ, Orme JP, Finlay MR, Ward RA, Mellor MJ, Hughes G, Rahi A, Jacobs VN, Red Brewer M, Ichihara E, Sun J, Jin H, Ballard P, Al-Kadhimi K, Rowlinson R, Klinowska T, Richmond GH, Cantarini M, Kim DW, Ranson MR, and Pao W (2014) AZD9291, an irreversible EGFR TKI, overcomes T790M-mediated resistance to EGFR inhibitors in lung cancer. *Cancer Discov* **4:**1046-1061.

de Vries NA, Buckle T, Zhao J, Beijnen JH, Schellens JH, and van Tellingen O (2012) Restricted brain penetration of the tyrosine kinase inhibitor erlotinib due to the drug transporters P-gp and BCRP. *Invest New Drugs* **30:**443-449.

Doroshow JH (2005) Targeting EGFR in non-small-cell lung cancer. *N Engl J Med* **353:**200-202.

Engelman JA, Zejnullahu K, Gale CM, Lifshits E, Gonzales AJ, Shimamura T, Zhao F, Vincent PW, Naumov GN, Bradner JE, Althaus IW, Gandhi L, Shapiro GI, Nelson JM, Heymach JV, Meyerson M, Wong KK, and Janne PA (2007) PF00299804, an irreversible pan-ERBB inhibitor, is effective in lung cancer models with EGFR and ERBB2 mutations that are resistant to gefitinib. *Cancer Res* **67:**11924-11932.

Franceschi E, Cavallo G, Lonardi S, Magrini E, Tosoni A, Grosso D, Scopece L, Blatt V, Urbini B, Pession A, Tallini G, Crino L, and Brandes AA (2007) Gefitinib in patients with progressive high-grade gliomas: a multicentre phase II study by Gruppo Italiano Cooperativo di Neuro-Oncologia (GICNO). *Br J Cancer* **96:**1047-1051.

Goss G, Tsai CM, Shepherd FA, Ahn MJ, Bazhenova L, Crino L, de Marinis F, Felip E, Morabito A, Hodge R, Cantarini M, Johnson M, Mitsudomi T, Janne PA, and Yang JC (2018) CNS response to osimertinib in patients with T790M-positive advanced NSCLC: pooled data from two phase II trials. *Ann Oncol* **29:**687-693.

Heffron TP (2016) Small Molecule Kinase Inhibitors for the Treatment of Brain Cancer. *J Med Chem* **59:**10030-10066.

Hoffknecht P, Tufman A, Wehler T, Pelzer T, Wiewrodt R, Schutz M, Serke M, Stohlmacher-Williams J, Marten A, Maria Huber R, Dickgreber NJ, and Afatinib Compassionate Use C (2015) Efficacy of the irreversible ErbB family blocker afatinib in epidermal growth factor receptor (EGFR) tyrosine kinase inhibitor (TKI)-pretreated non-small-cell lung cancer patients with brain metastases or leptomeningeal disease. *J Thorac Oncol* **10:**156-163.

Huang PH, Xu AM, and White FM (2009) Oncogenic EGFR signaling networks in glioma. *Sci Signal* **2:**re6.

Kalvass JC and Maurer TS (2002) Influence of nonspecific brain and plasma binding on CNS exposure: implications for rational drug discovery. *Biopharm Drug Dispos* **23:**327-338.

Kalvass JC, Phipps C, Jenkins GJ, Stuart P, Zhang X, Heinle L, Nijsen M, and Fischer V (2018) Mathematical and Experimental Validation of Flux Dialysis Method: An Improved Approach to Measure Unbound Fraction for Compounds with High Protein Binding and Other Challenging Properties. *Drug Metab Dispos* **46:**458-469.

Kawamura K, Yamasaki T, Yui J, Hatori A, Konno F, Kumata K, Irie T, Fukumura T, Suzuki K, Kanno I, and Zhang MR (2009) In vivo evaluation of P-glycoprotein and breast cancer resistance protein modulation in the brain using [(11)C]gefitinib. *Nucl Med Biol* **36:**239-246.

Krawczyk P, Kowalski DM, Ramlau R, Kalinka-Warzocha E, Winiarczyk K, Stencel K, Powrozek T, Reszka K, Wojas-Krawczyk K, Bryl M, Wojcik-Superczynska M, Glogowski M, Barinow-Wojewodzki A, Milanowski J, and Krzakowski M (2017) Comparison of the effectiveness of erlotinib, gefitinib, and afatinib for treatment of non-small cell lung cancer in patients with common and rare EGFR gene mutations. *Oncol Lett* **13:**4433-4444.

Kreisl TN, McNeill KA, Sul J, Iwamoto FM, Shih J, and Fine HA (2012) A phase I/II trial of vandetanib for patients with recurrent malignant glioma. *Neuro Oncol* **14:**1519-1526.

Levin VA (1980) Relationship of octanol/water partition coefficient and molecular weight to rat brain capillary permeability. *J Med Chem* **23:**682-684.

Liu X, Ding X, Deshmukh G, Liederer BM, and Hop CE (2012) Use of the cassette-dosing approach to assess brain penetration in drug discovery. *Drug Metab Dispos* **40:**963-969.

Lockman PR, Mittapalli RK, Taskar KS, Rudraraju V, Gril B, Bohn KA, Adkins CE, Roberts A, Thorsheim HR, Gaasch JA, Huang S, Palmieri D, Steeg PS, and Smith QR (2010) Heterogeneous blood-tumor barrier permeability determines drug efficacy in experimental brain metastases of breast cancer. *Clin Cancer Res* **16:**5664-5678.

Manitpisitkul P and White RE (2004) Whatever happened to cassette-dosing pharmacokinetics? *Drug Discov Today* **9:**652-658.

McCoach CE, Berge EM, Lu X, Baron AE, and Camidge DR (2016) A Brief Report of the Status of Central Nervous System Metastasis Enrollment Criteria for Advanced Non-Small Cell Lung Cancer Clinical Trials: A Review of the ClinicalTrials.gov Trial Registry. *J Thorac Oncol* **11:**407-413.

Minocha M, Khurana V, Qin B, Pal D, and Mitra AK (2012) Co-administration strategy to enhance brain accumulation of vandetanib by modulating P-glycoprotein (P-gp/Abcb1) and breast cancer resistance protein (Bcrp1/Abcg2) mediated efflux with m-TOR inhibitors. *Int J Pharm* **434:**306-314.

Ohgaki H and Kleihues P (2007) Genetic pathways to primary and secondary glioblastoma. *Am J Pathol* **170:**1445-1453.

Oldendorf WH (1974) Lipid solubility and drug penetration of the blood brain barrier. *Proc Soc Exp Biol Med* **147:**813-815.

Porta R, Sanchez-Torres JM, Paz-Ares L, Massuti B, Reguart N, Mayo C, Lianes P, Queralt C, Guillem V, Salinas P, Catot S, Isla D, Pradas A, Gurpide A, de Castro J, Polo E, Puig T, Taron M, Colomer R, and Rosell R (2011) Brain metastases from lung cancer responding to erlotinib: the importance of EGFR mutation. *Eur Respir J* **37:**624-631.

Raizer JJ, Abrey LE, Lassman AB, Chang SM, Lamborn KR, Kuhn JG, Yung WK, Gilbert MR, Aldape KD, Wen PY, Fine HA, Mehta M, Deangelis LM, Lieberman F, Cloughesy TF, Robins HI, Dancey J, Prados MD, and North American Brain Tumor C (2010) A phase I trial of erlotinib in patients with nonprogressive glioblastoma multiforme postradiation therapy, and recurrent malignant gliomas and meningiomas. *Neuro Oncol* **12:**87-94.

Rangachari D, Yamaguchi N, VanderLaan PA, Folch E, Mahadevan A, Floyd SR, Uhlmann EJ, Wong ET, Dahlberg SE, Huberman MS, and Costa DB (2015) Brain metastases in patients with EGFR-mutated or ALK-rearranged non-small-cell lung cancers. *Lung Cancer* **88:**108-111.

Rankovic Z (2015) CNS drug design: balancing physicochemical properties for optimal brain exposure. *J Med Chem* **58:**2584-2608.

Reardon DA, Conrad CA, Cloughesy T, Prados MD, Friedman HS, Aldape KD, Mischel P, Xia J, DiLea C, Huang J, Mietlowski W, Dugan M, Chen W, and Yung WK (2012) Phase I study of AEE788, a novel multitarget inhibitor of ErbB- and VEGF-receptor-family tyrosine kinases, in recurrent glioblastoma patients. *Cancer Chemother Pharmacol* **69:**1507-1518.

Reardon DA, Nabors LB, Mason WP, Perry JR, Shapiro W, Kavan P, Mathieu D, Phuphanich S, Cseh A, Fu Y, Cong J, Wind S, Eisenstat DD, Group BIT, and the Canadian Brain Tumour C (2015) Phase I/randomized phase II study of afatinib, an irreversible ErbB family blocker, with or without protracted temozolomide in adults with recurrent glioblastoma. *Neuro Oncol* **17:**430-439.

Riccardi K, Cawley S, Yates PD, Chang C, Funk C, Niosi M, Lin J, and Di L (2015) Plasma Protein Binding of Challenging Compounds. *J Pharm Sci* **104:**2627-2636.

Rich JN, Reardon DA, Peery T, Dowell JM, Quinn JA, Penne KL, Wikstrand CJ, Van Duyn LB, Dancey JE, McLendon RE, Kao JC, Stenzel TT, Ahmed Rasheed BK, Tourt-Uhlig SE, Herndon JE, 2nd, Vredenburgh JJ, Sampson JH, Friedman AH, Bigner DD, and Friedman HS (2004) Phase II trial of gefitinib in recurrent glioblastoma. *J Clin Oncol* **22:**133-142.

Sarkaria JN, Hu LS, Parney IF, Pafundi DH, Brinkmann DH, Laack NN, Giannini C, Burns TC, Kizilbash SH, Laramy JK, Swanson KR, Kaufmann TJ, Brown PD, Agar NYR, Galanis E, Buckner JC, and Elmquist WF (2018) Is the blood-brain barrier really disrupted in all glioblastomas? A critical assessment of existing clinical data. *Neuro Oncol* **20:**184-191.

Seshacharyulu P, Ponnusamy MP, Haridas D, Jain M, Ganti AK, and Batra SK (2012) Targeting the EGFR signaling pathway in cancer therapy. *Expert Opin Ther Targets* **16:**15-31.

Shinojima N, Tada K, Shiraishi S, Kamiryo T, Kochi M, Nakamura H, Makino K, Saya H, Hirano H, Kuratsu J, Oka K, Ishimaru Y, and Ushio Y (2003) Prognostic value of epidermal growth factor receptor in patients with glioblastoma multiforme. *Cancer Res* **63:**6962-6970.

Solca F, Dahl G, Zoephel A, Bader G, Sanderson M, Klein C, Kraemer O, Himmelsbach F, Haaksma E, and Adolf GR (2012) Target binding properties and cellular activity of afatinib (BIBW 2992), an irreversible ErbB family blocker. *J Pharmacol Exp Ther* **343:**342-350.

Togashi Y, Masago K, Fukudo M, Terada T, Fujita S, Irisa K, Sakamori Y, Kim YH, Mio T, Inui K, and Mishima M (2010) Cerebrospinal fluid concentration of erlotinib and its active metabolite OSI-420 in patients with central nervous system metastases of non-small cell lung cancer. *J Thorac Oncol* **5:**950-955.

van den Bent MJ, Brandes AA, Rampling R, Kouwenhoven MC, Kros JM, Carpentier AF, Clement PM, Frenay M, Campone M, Baurain JF, Armand JP, Taphoorn MJ, Tosoni A, Kletzl H, Klughammer B, Lacombe D, and Gorlia T (2009) Randomized phase II trial of erlotinib versus temozolomide or carmustine in recurrent glioblastoma: EORTC brain tumor group study 26034. *J Clin Oncol* **27:**1268-1274.

van Hoppe S, Sparidans RW, Wagenaar E, Beijnen JH, and Schinkel AH (2017) Breast cancer resistance protein (BCRP/ABCG2) and P-glycoprotein (P-gp/ABCB1) transport afatinib and restrict its oral availability and brain accumulation. *Pharmacol Res* **120:**43-50.

Wager TT, Hou X, Verhoest PR, and Villalobos A (2010) Moving beyond rules: the development of a central nervous system multiparameter optimization (CNS MPO) approach to enable alignment of druglike properties. *ACS Chem Neurosci* **1:**435-449.

Wager TT, Hou X, Verhoest PR, and Villalobos A (2016) Central Nervous System Multiparameter Optimization Desirability: Application in Drug Discovery. *ACS Chem Neurosci* **7:**767-775.

Weber B, Winterdahl M, Memon A, Sorensen BS, Keiding S, Sorensen L, Nexo E, and Meldgaard P (2011) Erlotinib accumulation in brain metastases from non-small cell lung cancer: visualization by positron emission tomography in a patient harboring a mutation in the epidermal growth factor receptor. *J Thorac Oncol* **6:**1287-1289.

Wind S, Giessmann T, Jungnik A, Brand T, Marzin K, Bertulis J, Hocke J, Gansser D, and Stopfer P (2014) Pharmacokinetic drug interactions of afatinib with rifampicin and ritonavir. *Clin Drug Investig* **34:**173-182.

Xiong S, Xue M, Mu Y, Deng Z, Sun P, and Zhou R (2017) Determination of AZD3759 in rat plasma and brain tissue by LC-MS/MS and its application in pharmacokinetic and brain distribution studies. *J Pharm Biomed Anal* **140:**362-366.

Yang Z, Guo Q, Wang Y, Chen K, Zhang L, Cheng Z, Xu Y, Yin X, Bai Y, Rabbie S, Kim DW, Ahn MJ, Yang JC, and Zhang X (2016) AZD3759, a BBB-penetrating EGFR inhibitor for the treatment of EGFR mutant NSCLC with CNS metastases. *Sci Transl Med* **8:**368ra172.

Yung WK, Vredenburgh JJ, Cloughesy TF, Nghiemphu P, Klencke B, Gilbert MR, Reardon DA, and Prados MD (2010) Safety and efficacy of erlotinib in first-relapse glioblastoma: a phase II open-label study. *Neuro Oncol* **12:**1061-1070.

Zeng Q, Wang J, Cheng Z, Chen K, Johnstrom P, Varnas K, Li DY, Yang ZF, and Zhang X (2015) Discovery and Evaluation of Clinical Candidate AZD3759, a Potent, Oral Active, Central Nervous System-Penetrant, Epidermal Growth Factor Receptor Tyrosine Kinase Inhibitor. *J Med Chem* **58:**8200-8215.

FOOTNOTES

This work was supported by the National Institutes of Health [Grants RO1 CA138437, RO1 NS077921, U54 CA210181, U01 CA227954 and P50 CA108960].

DMD Fast Forward. Published on January 31, 2019 as DOI: 10.1124/dmd.118.084210
This article has not been copyedited and formatted. The final version may differ from this version.

Legends for figures

Figure 1. Structures of EGFR inhibitors used in the current study.

Figure 2. Comparison of brain-to=plasma ratios between cassette and discrete dosing in wild-type and triple-knockout (Mdr1a/b$^{-/-}$Bcrp$^{-/-}$) FVB mice. (A) Brain-to-plasma ratios at 1-hour post dose in wild-type FVB mice. (B) Brain-to-plasma ratios at 8-hour post dose in wild-type FVB mice. (C) Brain-to-plasma ratios at 1-hour post dose in triple-knockout (Mdr1a/b$^{-/-}$Bcrp$^{-/-}$) FVB mice. (D) Brain-to-plasma ratios at 8-hour post dose in Mdr1a/b$^{-/-}$Bcrp$^{-/-}$ FVB mice.

Figure 3. Rank order of the brain distribution of EGFR inhibitors in a single animal. Rank order was based on the brain-to-plasma ratio at a single time point after dosing in individual animal.

Figure 4. Correlation between Kp and clogD/sqrt(MW) or MPO (multiparameter optimization) scores. (A) Correlation between Kp or Kpuu in wild-type FVB mice and clogD/sqrt(MW) (R square for Kp = 0.04895, R square for Kpuu = 0.224). (B) Correlation between Kp or Kpuu in triple-knockout (Mdr1a/b$^{-/-}$Bcrp$^{-/-}$) FVB mice and clogD/sqrt(MW) (R square for Kp = 0.137, R square for Kpuu = 0.0386). (C) Correlation between Kp or Kpuu in wild-type FVB mice and MPO score (R square for Kp = 0.108, R square for Kpuu = 0.0000911). (D) Correlation between Kp or Kpuu in triple-knockout (Mdr1a/b$^{-/-}$Bcrp$^{-/-}$) FVB mice and MPO score (R square for Kp = 0.557, R square for Kpuu = 0.433).

Table 1. physicochemical properties of EGFR inhibitors used in the study

Compound	Type	MW[b]	clogP[a]	clogD[a]	TPSA[b]	HBD[b]	pKa[a]	efflux liability
AEE788	Reversible[c]	441	4.44	3.49	60	2	8.24	Not reported
Afatinib	Irreversible[d]	486	3.76	2.34	89	2	8.81	P-gp and Bcrp[h]
AZD3759	NA	460	4.03	3.86	80	1	7.10	Not a substrate[l]
Dacomitinib	Irreversible[e]	470	4.71	3.53	79	2	8.55	Not reported
Erlotinib	Reversible[f]	393	3.20	3.20	75	1	4.62	P-gp and Bcrp[i]
Gefitinib	Reversible[f]	447	3.75	3.64	69	1	6.85	P-gp and Bcrp[j]
Osimertinib	Irreversible[g]	500	4.49	3.01	88	2	8.87	P-gp and Bcrp[h]
Vandetanib	NA	475	4.54	2.81	60	1	9.13	P-gp and Bcrp[k]

[a] obtained from ChemAxon (https://chemicalize.com/)

[b] obtained from PubChem (https://pubchem.ncbi.nlm.nih.gov/)

[c] (Reardon et al., 2012)

[d] (Solca et al., 2012)

[e] (Engelman et al., 2007)

[f] (Krawczyk et al., 2017)

[g] (Cross et al., 2014)

[h] (Ballard et al., 2016)

[i] (Agarwal et al., 2013)

[j] (Agarwal et al., 2010)

[k] (Minocha et al., 2012)

[l] (Zeng et al., 2015)

Table 2. PK parameters in wild-type mice

	unit	AEE788	Afatinib	AZD3759	Dacomitinib	Erlotinib	Gefitinib	Osimertinib	Vandetanib
t_{half}	hr	12.4	7.20	2.37	8.45	0.827	2.66	2.77	13.7
Apparent CL	mL/hr/kg	582	1196	1915	881	961	1706	1407	250
Apparent Vd	mL/kg	10377	12389	6539	10723	1146	6542	5632	4947
$t_{half, brain}$	hr	13.9	25.7*	2.69	10.5	0.75	14.2*	2.27	10.6
$AUC_{last, plasma}$	hr*ng/mL	985	734	486	826	1001	576	645	2230
$SE\_AUC_{last, plasma}$	hr*ng/mL	23.3	80.6	27.7	79.2	39.6	54.6	43.7	61.3
$AUC_{last, brain}$	hr*ng/mL	65.3	186	828	505	62.4	206	638	1416
$SE\_AUC_{last, brain}$	hr*ng/mL	2.20	3.35	60.8	24.0	8.21	3.85	31.9	95.0

t_{half}, half-life of a drug in plasma

Apparent CL, apparent clearance CL/F

Apparent Vd, Apparent volume of distribution, Vd/F

$t_{half, brain}$, half-life of a drug in brain

$AUC_{last, plasma}$, area under the curve from zero to the time of last measured concentration in plasma

$SE\_AUC_{last, plasma}$, standard error of an estimate of area under the curve in plasma

$AUC_{last, brain}$, area under the curve from zero to the time of last measured concentration in brain

$SE\_AUC_{last, brain}$, standard error of an estimate of area under the curve in brain

* the half-life was determined by the slope of last three time points in concentration-time profile.
The values were larger than the half-life in plasma because complete elimination phase has not been captured in the experiments.

Table 3. PK parameters in TKO mice

	unit	AEE788	Afatinib	AZD3759	Dacomitinib	Erlotinib	Gefitinib	Osimertinib	Vandetanib
t_{half}	hr	17.6	5.95	2.75	8.99	0.846	4.20	2.24	5.74
Apparent CL	mL/hr/kg	531	679	1598	822	1570	1431	1657	614
Apparent Vd	mL/kg	13502	5827	6349	10667	1916	8680	5353	5085
$t_{half,brain}$	hr	5.1	10.5	2.32	16.6	0.95	4.76	3.59	41.8*
$AUC_{last,\ plasma}$	hr*ng/mL	858	1279	617	877	609	658	566	1442
$SE\_AUC_{last,\ plasma}$	hr*ng/mL	61.8	234	95.9	135	49.7	95.3	81.6	98.7
$AUC_{last,\ brain}$	hr*ng/mL	1599	3082	1633	8572	124	1449	8913	10773
$SE\_AUC_{last,\ brain}$	hr*ng/mL	89.1	174	72.0	307	6.12	57.0	1584	563

t_{half}, half-life of a drug in plasma

Apparent CL, apparent clearance CL/F

Apparent Vd, Apparent volume of distribution, Vd/F

$t_{half,\ brain}$, half-life of a drug in brain

$AUC_{last,\ plasma}$, area under the curve from zero to the time of last measured concentration in plasma

$SE\_AUC_{last,\ plasma}$, standard error of an estimate of area under the curve in plasma

$AUC_{last,\ brain}$, area under the curve from zero to the time of last measured concentration in brain

$SE\_AUC_{last,\ brain}$, standard error of an estimate of area under the curve in brain

* the half-life was determined by the slope of last three time points in concentration-time profile.
The values were larger than the half-life in plasma because complete elimination phase has not been captured in the experiments.

Table 4. The partition coefficients and free partition coefficients of brain for EGFR inhibitors.

	AEE788	Afatinib	AZD3759	Dacomitinib	Erlotinib	Gefitinib	Osimertinib	Vandetanib
Kp,brain, wild-type	0.066	0.254	1.70	0.612	0.062	0.358	0.988	0.635
Kp,brain, TKO	1.86	2.41	2.65	9.77	0.204	2.20	15.7	7.47
fu,p	0.068	0.080	0.058	0.008	0.045	0.041	0.005	0.055
fu,b	0.029	0.014	0.101	0.007	0.096	0.012	0.001	0.012
Kp,uu, wild-type	0.029	0.046	2.96	0.493	0.134	0.103	0.289	0.138
Kp,uu, TKO	0.804	0.433	4.61	7.88	0.438	0.631	4.61	2.65
DA	28.1	9.49	1.56	16.0	3.27	6.16	15.9	19.1

Kp (AUC ratio), the ratio of $AUC_{last,\ brain}$ to $AUC_{last,\ plasma}$ using total drug concentrations

Kp,uu (AUC ratio), the ratio of $AUC_{last,\ brain}$ to $AUC_{last,\ plasma}$ using free drug concentrations

$f_{u,p}$, free fraction in plasma measured by rapid equilibrium dialysis (n=4)

$f_{u,b}$, free fraction in brain homogenate measured by rapid equilibrium dialysis (n=4)

DA, distribution advantage calculated by the ratios of Kp,brain in trangenic to Kp,brain in wild-type

Table 5. The calculated scores based on physicochemical properties and the partition coefficients of brain

Compound	CNS MPO Score[a]	cLogD/ sqrt(MW)	Kp_{brain} in publication	Kp_{brain} in wild-type	$Kp_{uu,\ brain}$ in wild-type	Kp_{brain} in TKO	$Kp_{uu,\ brain}$ in TKO	DA
AEE788	3.3	0.166	NA	0.066	0.029	1.86	0.80	28
Afatinib	3.6	0.106	0.35[d]	0.268	0.048	2.41	0.43	9
AZD3759	3.7	0.180	0.89[e]	1.70	2.96	2.65	4.61	2
Dacomitinib	2.8	0.163	NA	0.612	0.493	9.77	7.88	16
Erlotinib	4.9	0.161	0.02[f]/0.14[g]	0.060	0.130	0.20	0.44	3
Gefitinib	4.0	0.172	0.21[h]/0.3[i]	0.358	0.103	2.20	0.63	6
Osimertinib	2.8	0.135	1.78[j]	0.988	0.289	15.7	4.61	16
Vandetanib	3.3	0.129	0.21[k]	0.635	0.138	12.2	2.65	19

[a] MPO, multiparameter optimization score calculated by using the method from (Wager et al., 2016)
[d] reported from (van Hoppe et al., 2017)
[e] reported from (Xiong et al., 2017)
[f] in rat. Reported from (Agarwal et al., 2013)
[g] in mouse. Reported from (de Vries et al., 2012)
[h] in nude mice. Reported from (Ballard et al., 2016)
[i] in FVB mice. Reported from (Agarwal et al., 2010)
[j] in nude mice. Reported from (Ballard et al., 2016)
[k] in FVB mice. Reported from (Minocha et al., 2012)

Table 6. Summary of clinical information on the studied 8 EGFR inhibitors

Compound	Clinical status	Dose in patients (mg/day)	Brain penetration (% of CSF to plasma levels) in patient	Brain penetration (% of brain to plasma ratio) in pre-clinical model	Response rate in patients with primary brain tumor (%)	Response rate in patients with brain metastases (%)	References
AEE788	Terminated	50 - 800	ND	ND	GBM, stable disease (17%)	ND	(Reardon et al., 2012)
Afatinib	Giotrif	50	0.7	ND	GBM, stable disease (14%)	35%	(Wind et al., 2014; Hoffknecht et al., 2015; Reardon et al., 2015)
AZD3759	Phase I (fast review)	100-1000	111	282	ND	83%	(Zeng et al., 2015; Ahn et al., 2017; Xiong et al., 2017)
Dacomitinib	Phase 2-3	45/60	NA	NA	ND	6.3 %[a]	
Erlotinib	Tarceva	150	2.77- 5.1	13.7	GBM, PFS6 (3%) first-relapse GBM, OR (6.3%)	82.4 (EGFR mutation)	(Raizer et al., 2010; Togashi et al., 2010; Yung et al., 2010; Porta et al., 2011; de Vries et al., 2012)
Gefitinib	Iressa	750-1000	1.07-3.58	27	astrocytoma, overall disease-control rate (17.9%) GBM, overall disease-control rate (12.5%)	27%	(Ceresoli et al., 2004; Franceschi et al., 2007; Chen et al., 2013)
Osimertinib	Tagrisso	80	NA	180	ND	54% (T790M+)	(Ballard et al., 2016; Goss et al., 2018)
Vandetanib	Caprelsa	300	1.2 - 2.4	21	GBM, objective response rate (12.5%)	ND	(Kreisl et al., 2012)

[a] from clinicaltrials.gov (identifier: NCT01858389)

GBM (glioblastoma); ND (not determined); NA (not available); PFS6 (progression-free survival at 6 months); OR (objective rate)

DMD Fast Forward. Published on January 31, 2019 as DOI: 10.1124/dmd.118.084210
This article has not been copyedited and formatted. The final version may differ from this version.

Figure 1. Structures of EGFRi used in the current study

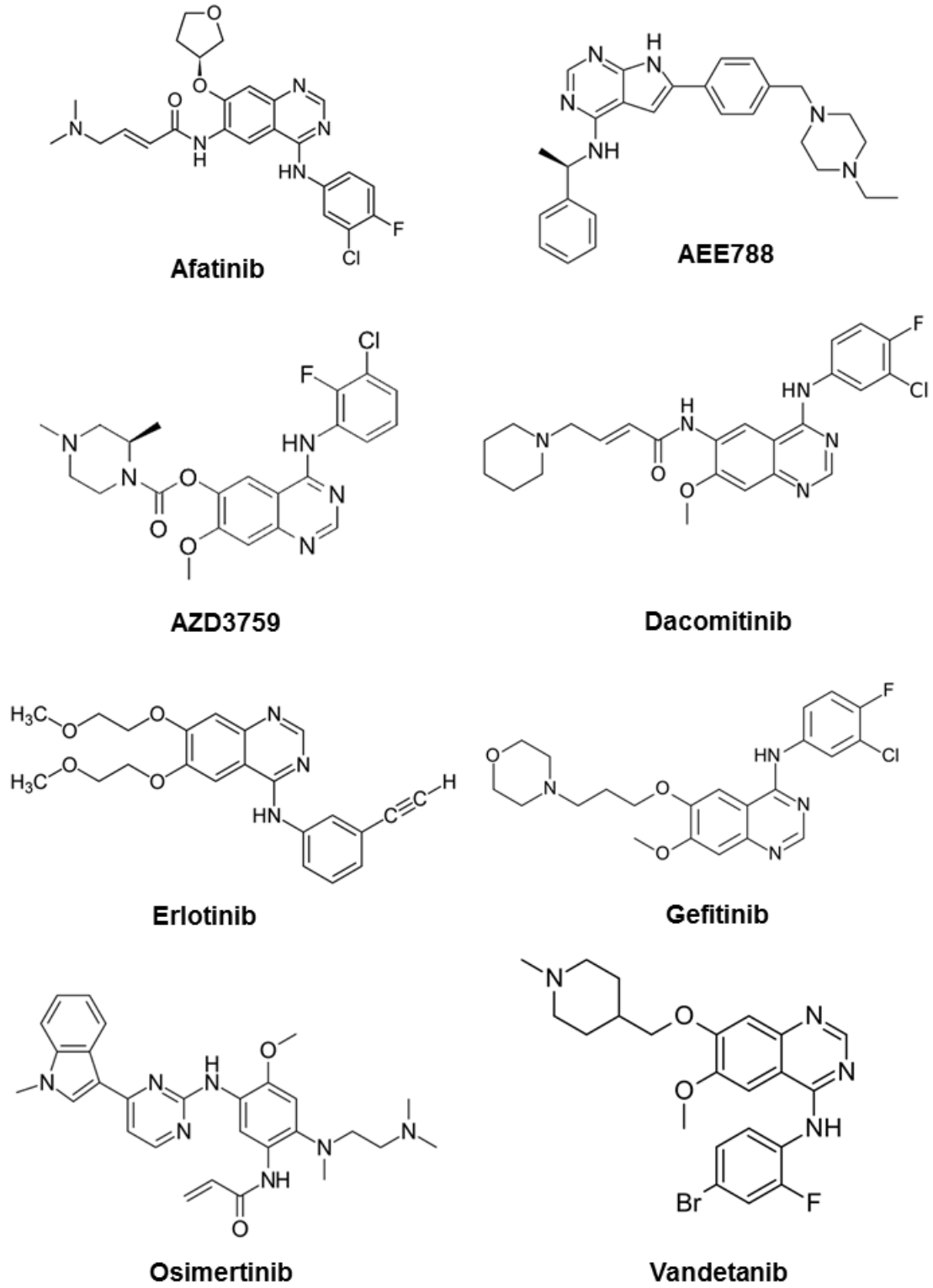

DMD Fast Forward. Published on January 31, 2019 as DOI: 10.1124/dmd.118.084210
This article has not been copyedited and formatted. The final version may differ from this version.

Figure 2. Comparison of brain-to-plasma ratio between cassette and discrete dosing in wild-type and Mdr1a/b$^{-/-}$Bcrp1$^{-/-}$ FVB mice.

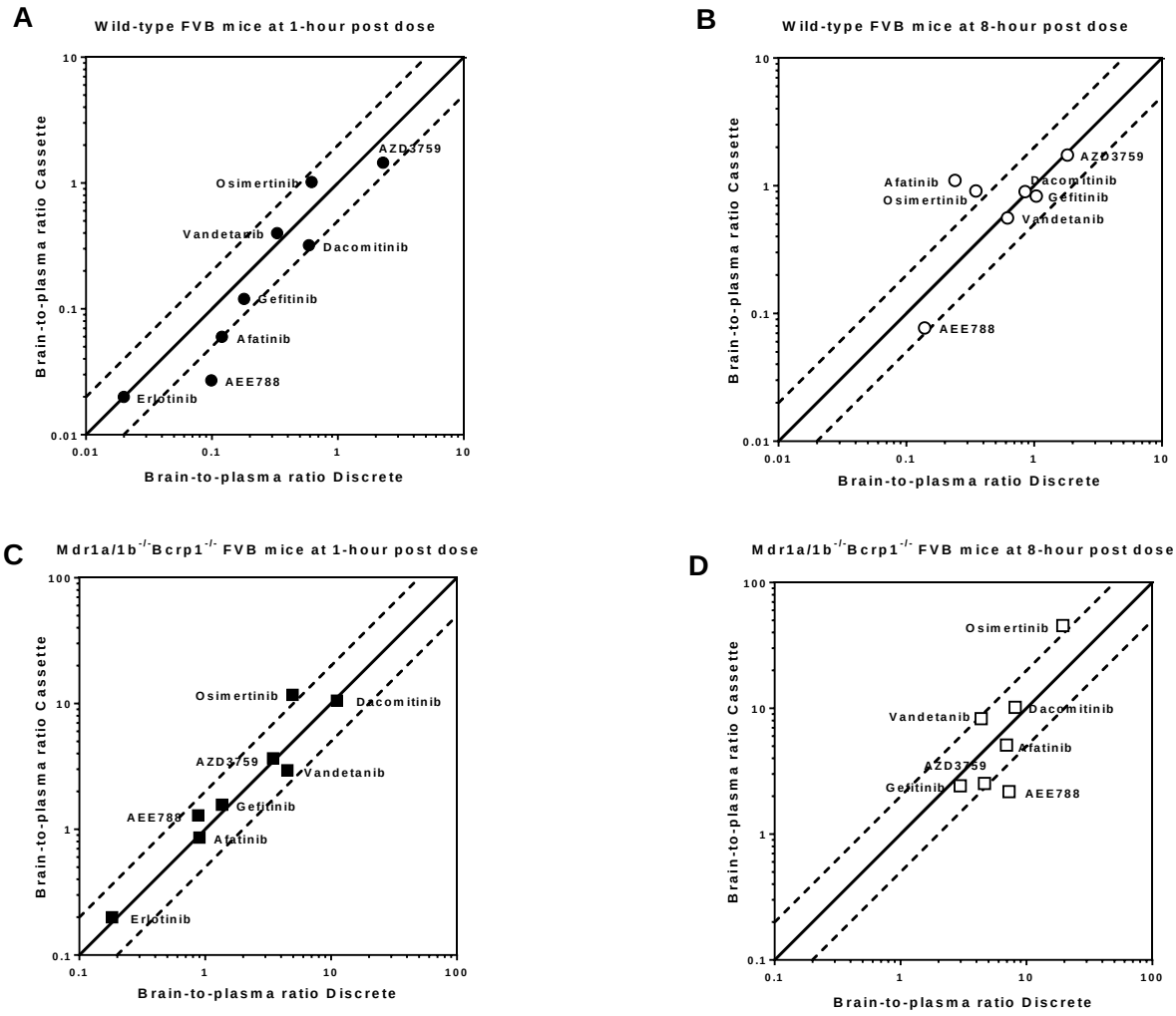

DMD Fast Forward. Published on January 31, 2019 as DOI: 10.1124/dmd.118.084210
This article has not been copyedited and formatted. The final version may differ from this version.

Figure 3. Rank order of EGFR inhibitor brain distribution with a single animal

A. Rank order in wild-type (WT) mice

Animal ID	Time of Collection	Erlotinib	AEE788	Afatinib	Gefitinib	Dacomitinib	Vandetanib	Osimertinib	AZD3759	
1	0.5h	0.031	0.030	0.121	0.135	0.491	0.302	0.789	0.357	1
2	0.5h	0.027	0.061	0.038	0.130	0.266	0.424	0.566	1.97	2
3	0.5h	0.029	0.031	0.070	0.119	0.174	0.302	0.716	1.67	3
4	0.5h	0.027	0.031	0.032	0.115	0.209	0.295	0.239	1.48	4
5	1h	0.016	0.021	0.022	0.071	0.399	0.355	0.597	1.09	5
6	1h	0.022	0.028	0.059	0.129	0.494	0.333	1.06	1.32	6
7	1h	0.028	0.044	0.070	0.167	0.243	0.607	1.44	2.04	7
8	1h	0.018	0.016	0.044	0.104	0.139	0.314	1.00	1.35	8
9	2h	0.015	0.060	0.147	0.166	1.76	0.347	1.59	1.45	
10	2h	0.028	0.094	0.207	0.216	1.43	0.337	1.73	1.53	
11	2h	0.018	0.046	0.055	0.104	ND	0.739	1.23	1.77	
12	2h	0.017	0.046	0.078	0.128	ND	0.494	0.950	1.08	
13	4h	0.020	0.084	0.165	0.229	0.593	0.816	1.95	1.37	
14	4h	0.027	0.092	0.417	0.195	0.359	0.570	1.80	1.97	
15	4h	2.68	0.084	0.483	0.359	0.435	1.34	1.44	1.95	
16	4h	LLOQ	0.098	0.481	0.658	0.623	1.16	1.14	2.00	
17	8h	LLOQ	0.074	1.03	LLOQ	1.12	0.538	0.485	2.32	
18	8h	LLOQ	0.081	0.970	1.30	1.17	0.509	0.798	1.94	
19	8h	LLOQ	0.070	1.07	0.677	0.361	0.606	1.25	1.54	
20	8h	LLOQ	0.082	1.32	0.498	0.946	0.588	1.10	1.15	
21	16h	LLOQ	0.073	1.11	LLOQ	LLOQ	0.571	0.159	5.45	
22	16h	LLOQ	0.071	LLOQ	3.78	1.01	LLOQ	LLOQ	LLOQ	
23	16h	LLOQ	0.084	1.08	3.97	0.586	0.732	0.050	2.17	
24	16h	LLOQ	0.077	1.34	2.47	0.193	0.793	0.104	21.2	

B. Rank order in Mdr1a/b$^{-/-}$Bcrp1$^{-/-}$ (Triple knockout, TKO) mice

Animal ID	Time of Collection	Erlotinib	Afatinib	AEE788	Gefitinib	AZD3759	Vandetanib	Dacomitinib	Osimertinib	
1	0.5h	0.423	0.562	1.85	0.897	1.33	1.74	3.09	5.71	1
2	0.5h	0.167	0.468	0.574	1.00	2.90	1.64	4.05	5.84	2
3	0.5h	0.159	0.193	0.658	0.661	2.18	2.45	14.2	8.27	3
4	0.5h	0.131	0.583	0.621	0.92	2.97	1.81	11.3	3.06	4
5	1h	0.258	1.14	1.21	1.39	3.10	3.70	ND	17.7	5
6	1h	0.179	1.15	1.08	1.38	3.04	2.72	5.88	5.55	6
7	1h	0.217	0.272	1.43	2.01	5.94	3.03	4.19	20.0	7
8	1h	0.147	0.875	1.45	1.50	2.59	2.37	21.6	3.67	8
9	2h	0.354	1.94	2.63	2.52	4.39	3.10	12.4	7.66	
10	2h	0.164	1.10	4.65	4.73	5.66	7.15	16.4	23.1	
11	2h	0.278	1.86	1.53	1.49	2.45	4.66	10.5	3.58	
12	2h	0.201	1.16	0.943	1.33	2.11	4.57	4.93	20.0	
13	4h	4.18	3.11	2.69	2.39	2.66	8.01	24.1	52.3	
14	4h	0.150	3.43	4.20	2.77	2.43	8.29	19.3	19.9	
15	4h	0.057	2.55	3.42	3.25	3.48	5.83	23.7	16.3	
16	4h	0.915	7.97	2.20	6.65	19.2	7.19	17.1	10.3	
17	8h	LLOQ	0.944	1.22	0.96	0.42	13.5	18.5	LLOQ	
18	8h	LLOQ	2.11	1.99	2.22	2.28	6.04	11.3	46.7	
19	8h	LLOQ	6.71	3.07	3.30	2.65	41.8	28.2	64.5	
20	8h	LLOQ	6.51	2.46	3.22	2.67	5.30	12.0	25.3	
21	16h	LLOQ	3.21	0.773	2.23	0.766	23.3	6.24	5.18	
22	16h	LLOQ	6.41	0.921	3.69	11.4	LLOQ	LLOQ	LLOQ	
23	16h	LLOQ	8.59	0.713	11.3	LLOQ	LLOQ	LLOQ	LLOQ	

DMD Fast Forward. Published on January 31, 2019 as DOI: 10.1124/dmd.118.084210
This article has not been copyedited and formatted. The final version may differ from this version.

Figure 4. Correlation between Kp and clogD/sqrt(MW) or MPO score in wild-type and TKO.

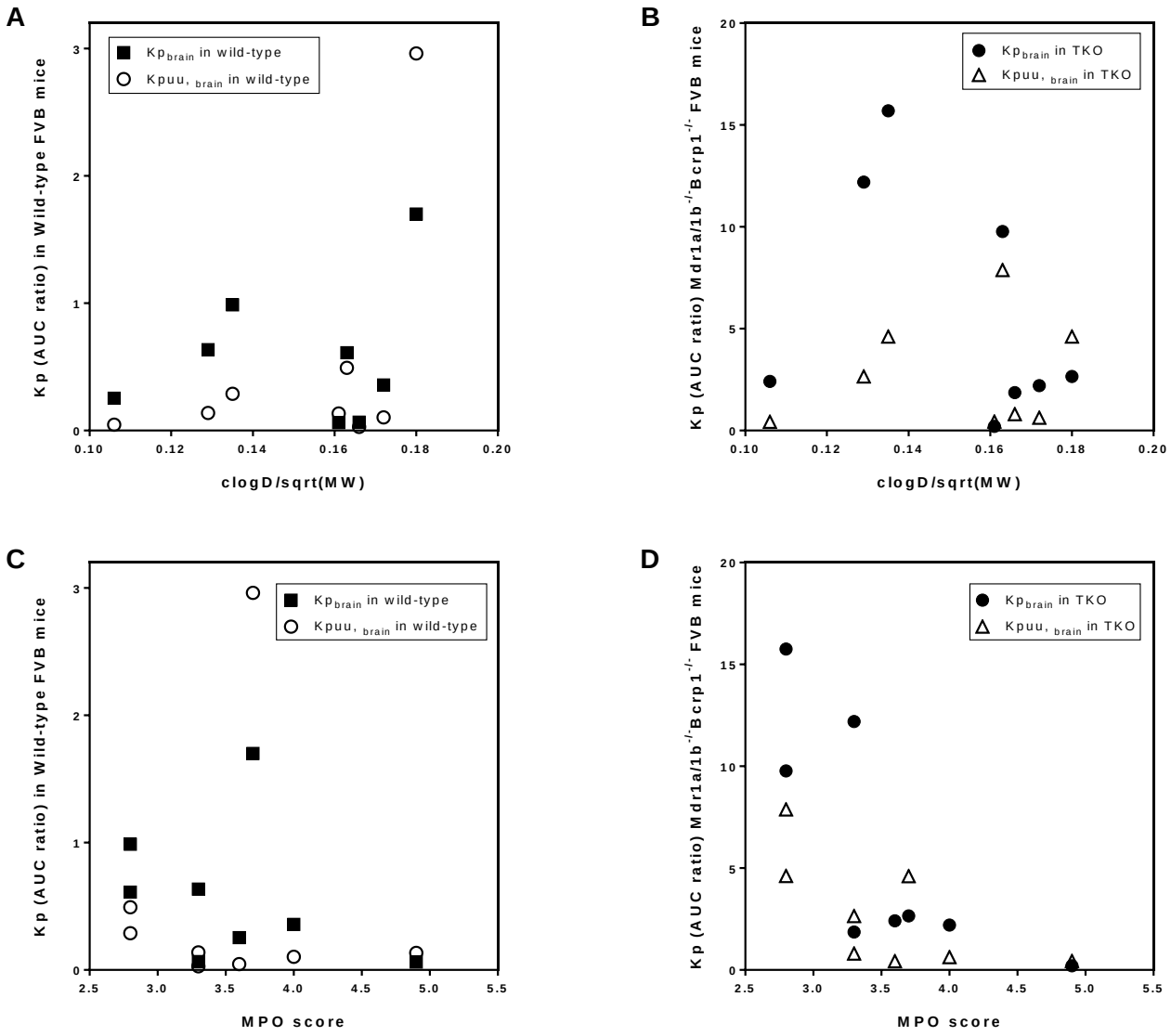

DMD Fast Forward. Published on January 31, 2019 as DOI: 10.1124/dmd.118.084210
This article has not been copyedited and formatted. The final version may differ from this version.